

Effects of rail joints and train's critical speed on the dynamic behavior of bridges

Y. Khadri*, S. Tekili**, E. M. Daya***, A. Daouadji****, B. Merzoug*****

*Université Badji Mokhtar, LMI, BP12- Annaba, Algeria, E-mail: khadri@univ-metz.fr

**Université Badji Mokhtar, LMI, BP12- Annaba, Algeria, E-mail: tekili_s@yahoo.fr

***Université de Lorraine, LEM3- Metz, Ile du Saulcy, 57045 Metz, France, E-mail:-daya@univ-metz.fr

****Université de Lorraine, LEM3- Metz, Ile du Saulcy, 57045 Metz, France, E-mail: daouadji@univ-metz.fr

*****Université Badji Mokhtar, LMI, BP12- Annaba, Algeria, E-mail: merzougbachir@yahoo.fr

crossref <http://dx.doi.org/10.5755/j01.mech.19.1.3615>

1. Introduction

Bridge response is defined in terms of the dynamic amplification factor (*DAF*), which is the ratio of the maximum response resulting from moving loads, to the maximum static response. Determining the real *DAF* is not easy; it depends on important parameters such as the bridge's geometrical properties and the roughness of the rails. For this reason, there is no international consensus on the calculation of the *DAF* and divergences exist between the recommendations of various standards and codes in the dimensioning of bridges. The first study developed analytical solutions for simple cases of moving forces on a beam with two simple supports [1]. Certain authors propose solutions to solve the case of a mass moving over the beam with various supports configurations [2]. For arch bridges traversed by a single moving load, [3] use a mixed approach in which the advantages of continuum and lumped mass methods have been combined. On the other hand, [4] determined the dynamic responses of a circular curved Timoshenko beam caused by a moving load using the curved beam elements. Thereafter, a discrete mechanical system was employed for a better representation of the vehicle movement [5]; the case of a convoy of vehicles was studied. The simplest model made up of a rigid block with three degrees of freedom gives results similar to the models having more degrees of freedom [6]. Studies of experimental codes carried out on bridges [7] aimed to determine the principal dynamic characteristics of the bridge: they constitute an excellent means to study the phenomena of interaction between the vehicle and the bridge; nevertheless they do not make it possible to conduct complete parametric studies. The studies by [5] and [8] modeled the dynamic behavior of the bridges using finite element programs. There are very few published investigations of joints in track. In [9], it was sought to obtain rail joints with a better mechanism by analyzing the outcome of the rail joints using continuously welded rails along with a vertical load.

For the study of certain parameters, the numerical analysis is more attractive despite the problems of adequately modeling the complex phenomenon of the dynamic interaction between the vehicles and the bridge. The dynamic behavior of the bridge is carried out through a parametric study for various speeds, for different rail roughness conditions, and for various defect of the rail (joint).

2. Dynamic model of a train-bridge interaction system

2.1. Rail profile generation

Then roughness profile of the rail in its discrete form is given by [10]:

$$r_r = \sum_{k=1}^N \sqrt{4A_r \left(\frac{2\pi k}{L_c \omega_{s0}} \right)^{-2} \frac{2\pi}{L_c} \cos(\omega_{sk}x - \varphi_k)}, \quad (1)$$

where A_r is the roughness coefficient in m^3/cycle , ω_{s0} is the discontinuity frequency equal to $1/2\pi$ (cycle/m), $\omega_{sk} = 2\pi k/L_c$ and L_c is, in general, twice the length of the bridge. The phase angle φ_k is produced by a generator of random numbers. In general, random sampling algorithms are based on the use of random numbers ζ uniformly distributed. Among the "good" random number generators currently available, the simplest ones are the so-called multiplicative congruential generators [11]. A popular example of this type of generator is the following:

$$\xi_n = R_n / (2^{31} - 1). \quad (2)$$

This provides a sequence of random numbers ξ_n uniformly distributed in $[0, 1]$ from a given seed $R_0 < 2^{31} - 1$:

$$R_n = 7^{31} R_{n-1} \bmod (2^{31} - 1). \quad (3)$$

The generator (2) is known to have good random properties. However, the sequence is periodic, with a period on the order of approximately 10^9 .

2.2. Modeling of rail joints

The train/track model can simulate many defects such as rails with a crushed head, fatigue-damaged rails, rail joints, surface roughness, corrugated rails, (Fig. 1) etc. The rail joints always have a space between two consecutive rails to adapt to the dilation and the shrinking of the material caused by variations in temperature. In this paper, only rail roughness and rail joints are investigated. The joints between the rails are modeled by singular and periodic irregularities. The rail joint model is shown in Fig. 2.

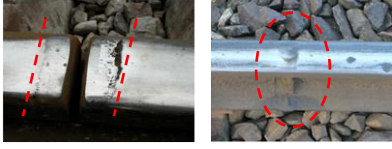


Fig. 1 Rail defects: Insulated rail joint with wide gap (left) and rail weld (right)

The joint profile can be mathematically expressed by the following function:

$$r_d(x) = \begin{cases} \frac{1}{2}a \left(1 - \cos\left(\frac{2\pi(x-C)}{b}\right) \right) & \text{for } C \leq x \leq C+b \\ 0 & \text{elsewhere,} \end{cases} \quad (4)$$

where $C = B + k(b + A)$, $k = 0, 1, 2, \dots, N_j$, a , b denote the depth and length of the joint, respectively, A is the rail length between two joints, B is the distance from the origin to the first joint, $N_j = (L - B)/(A + b)$ is the joint number.

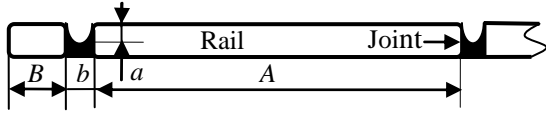


Fig. 2 Model of rail joints defect

To the roughness profile of the rail (Eq. 1), one can superimpose other curves representing singular irregularities or periodic defects (Eq. 4):

$$r(x) = r_r(x) + r_d(x). \quad (5)$$

2.3. Train model

Consider a simply supported beam subjected to a high-speed train. The bridge is modeled by Euler-Bernoulli beam [12]. Fig. 3 shows a train that is modeled by a set of identical cars with a constant spacing, and moving at a constant speed, v , over a bridge. The vehicle is composed of two masses, the one at the top representing the mass of the car body, m_v , and the one at the bottom representing the mass of the wheel assembly m_s (Fig. 3, b) [13]. The two masses are connected by a spring and dashpot to account for the vehicle suspension (system with 2DOF).

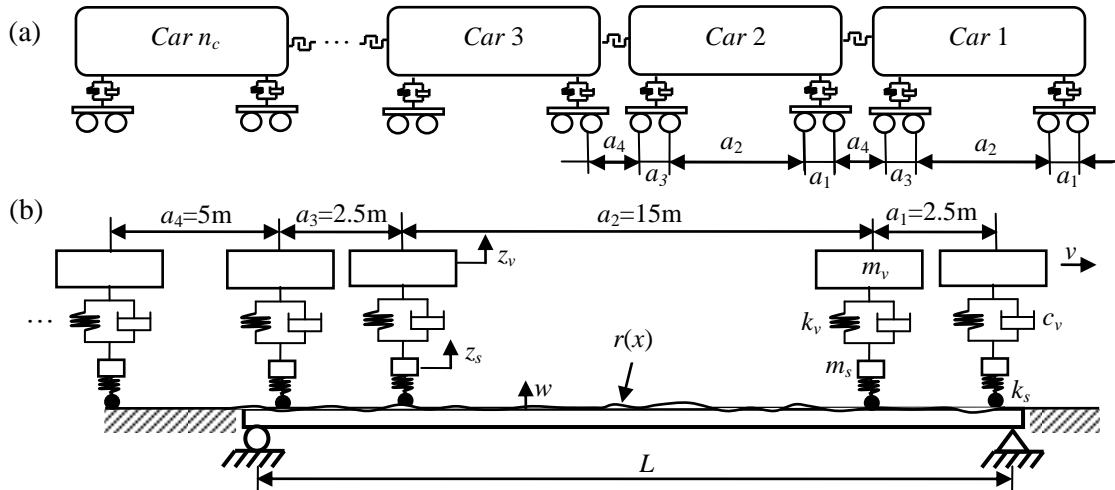


Fig. 3 Model of bridge-train: a) high-speed train, b) a series of systems with two degrees of freedom

The dynamic equilibrium equations of m_s and m_v are as follows [13] (Fig. 4):

$$m_s \ddot{z}_s = c_v (\dot{z}_v - \dot{z}_s) + k_v (z_v - z_s) - k_s \Delta; \quad (6)$$

$$m_v \ddot{z}_v = c_v (\dot{z}_s - \dot{z}_v) + k_v (z_s - z_v), \quad (7)$$

where k_v the vertical stiffness of primary suspension, c_v is the damping of the primary suspension, z_v is the vertical displacement of the mass m_v , k_s is the rigidity of wheel suspension.

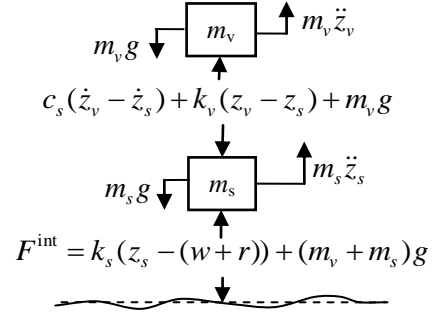


Fig. 4 Dynamic rolling systems with two degrees of freedom vehicle

The relative vertical displacement between the i th wheel and the bridge is $\Delta_i = -z_s + w + r$ where z_s is the vertical displacement of the i th wheel, r is the rail roughness under the i th wheel and w is the bridge vertical displacement under the i th wheel.

2.4. Bridge model

Only a single span of this simply supported multi-girder highway bridge is considered in order to study the DAF under the action of a moving vehicle. We can use the well-known Lagrangian formulation with the Lagrangian function $L = V - U$ and

$$\frac{d}{dt} \left(\frac{\partial L}{\partial \dot{q}_j} \right) - \frac{\partial L}{\partial q_j} = \sum_{k=1}^{n_v} \delta(x - x_k) F_j(t), \quad j = 1, 2, \dots, n, \quad (8)$$

where n_v is the number of forces applied to the bridge

(number of the cars), δ is the Dirac function, V is the kinetic energy, and U is the potential energy. Their expressions are given in [13]. The $F_j(t)$ is the generalized force. The position of the force on the bridge can be calculated as follows with $a_0 = 0$:

$$x_k = x_l - \sum_{l=1}^{k-1} a_l. \quad (9)$$

Employing the modal analysis method, the bridge deflection can be approximated by a series of n sinusoidal modes:

$$w(x, t) = \sum_{j=1}^n q_j(t) \phi_j(x_k(t)), \quad (10)$$

where $\phi_j(x_k(t)) = \sin(j\pi x/L)$ is the shape of the j th beam mode, for a simply supported beam and the circular frequency is given by:

$$\omega_j = (j\pi/L)^2 \sqrt{EI/m_l}. \quad (11)$$

The term in Eq. (10) and (11) are: $q_j(t)$ the generalized coordinates of the system, n the number of the adopted vibration modes, E the Young modulus, I the moment of inertia, and m_l the mass per unit length.

The projection of the Eq. (8), in the modal space [14] is given by:

$$\sum_{j=1}^n m_{ij} \ddot{q}_j + \sum_{j=1}^n c_{ij} \dot{q}_j + \sum_{j=1}^n k_{ij} q_j = P_j(t) - \sum_{k=1}^{n_v} m_v \phi_i(x_k(t)) \ddot{z}_v - \sum_{k=1}^{n_s} m_s \phi_i(x_k(t)) \ddot{z}_s \quad i = 1, 2, \dots, n, \quad (12)$$

where:

$$P_j(t) = - \sum_{k=1}^{n_v} \frac{2}{m_l L} (m_v + m_s) g \phi_j(x_k(t)) \quad i = 1, 2, \dots, n. \quad (13)$$

From Eqs. (6), (7) and (12) the problem can be introduced by the following matrix formulation:

$$\begin{bmatrix} M & \Phi M_s & \Phi M_v \\ 0 & M_s & 0 \\ 0 & 0 & M_v \end{bmatrix} \begin{Bmatrix} \ddot{q} \\ \ddot{z}_s \\ \ddot{z}_v \end{Bmatrix} + \begin{bmatrix} C & 0 & 0 \\ 0 & C_v & -C_v \\ 0 & -C_v & C_v \end{bmatrix} \begin{Bmatrix} \dot{q} \\ \dot{z}_s \\ \dot{z}_v \end{Bmatrix} + \begin{bmatrix} K & 0 & 0 \\ -K_s \Phi^T & K_v + K_s & -K_v \\ 0 & -K_v & K_v \end{bmatrix} \begin{Bmatrix} q \\ z_s \\ z_v \end{Bmatrix} = \begin{Bmatrix} P \\ K_s r(x(t)) \\ 0 \end{Bmatrix}, \quad (14)$$

where the sub-matrices and sub-vectors are given below:

$$\left. \begin{aligned} M &= [\delta_{ij}], \quad C = [2\xi_j \omega_j \delta_{ij}], \quad K = [\omega_j^2 \delta_{ij}], \\ M_v &= \text{diag}[m_{vk}], \quad C_v = \text{diag}[c_{vk}], \quad K_v = \text{diag}[k_{vk}], \\ M_s &= \text{diag}[m_{sk}], \quad K_s = \text{diag}[m_{sk}], \quad q = \{q_j\}^T, \\ z_v &= \{z_{vk}\}^T, \quad z_s = \{z_{sk}\}^T, \quad P = \{P_j\}^T, \quad r = \{r(x_k(t))\}^T, \\ \Phi &= [\phi_i(x_k(t))], \quad i, j = 1, 2, \dots, n, \quad k = 1, 2, \dots, n_v. \end{aligned} \right\} \quad (15)$$

The system of differential Eq. (14) can be solved with different integration techniques. In this work, the Eq. (14) are solved using implicit Newmark integration scheme [15] and $\Delta t = 0.25e-3$ s. This method yields a stable and accurate solution, with Newmark's parameters $\gamma = 0.5$ and $\beta = 0.25$. By solving this equation, the displacement of the vehicle and bridge can be obtained as a function of time. We propose a numerical algorithm (Fig. 5) to solve the problem of the bridge-vehicle interaction. The algorithm is composed of two overlapping loops: the first one for the time-steps, the second corresponds to the number of vehicles. The dynamic response of the bridge is estimated by superposition of the modes up to the 10th. A computer program in FORTRAN is developed for the analysis of railways defects on the dynamic response of a bridge. Both the DAF , and the speed parameter α , which are dimensionless, are useful parameters in analyzing the vehicle induced vibrations. The dynamic effects induced by the moving train on the railway bridge were investigated by computing the dynamic amplification factor, defined as:

$$DAF = R_d(x)/R_s(x), \quad (16)$$

where $R_d(x)$ is the maximum dynamic displacement and $R_s(x)$ is the maximum static displacement (null speed) at the mid-span of the bridge.

The dimensionless frequency parameter α is defined as the ratio of the excitation frequency of the moving train, to the natural frequency of vibrations of the bridge, as:

$$\alpha = f_v / f_B. \quad (17)$$

The applied load frequency f_v (trainload frequency) is given by the following equation [5]:

$$f_v = \frac{kv}{d}, \quad k = 1, 2, 3, \dots, \quad (18)$$

where v is the train speed and d is the carriage length.

When f_v equals f_B ($\alpha = 1$), the resonance of the bridge and trainload is obvious. The critical speeds, v_{cr} to resonate under the passage of the train are provided by [16]:

$$v_{cr} = \frac{d f_{Bj}}{k}, \quad j = 1, 2, \dots, n, \quad k = 1, 2, 3, \dots, \quad (19)$$

where $f_{Bj} = \omega_j / 2\pi$ is natural frequency of the bridge and the carriage length is $d = a_1 + a_2 + a_3 + a_4$.

3. Validation test

To validate the present algorithm (Fig. 5), a simple example is considered (Fig. 6), which has been studied by several authors [2, 8]. As shown in Fig. 6, a simple beam of span length $L = 25$ m is subjected to a moving mass-spring. The flowing data are adopted [8]: Young's modulus $E = 2.87$ GPa; The flowing data are adopted [8]: span length $L = 25$ m; Young's modulus $E = 2.87$ GPa; moment of inertia $I = 2.90$ m⁴, mass per unit length $m_l = 2303$ kg/m, suspended mass $m_v = 5750$ kg, suspension stiffness $k_v = 1595$ kN/m, and speed $v = 27.78$ m/s.

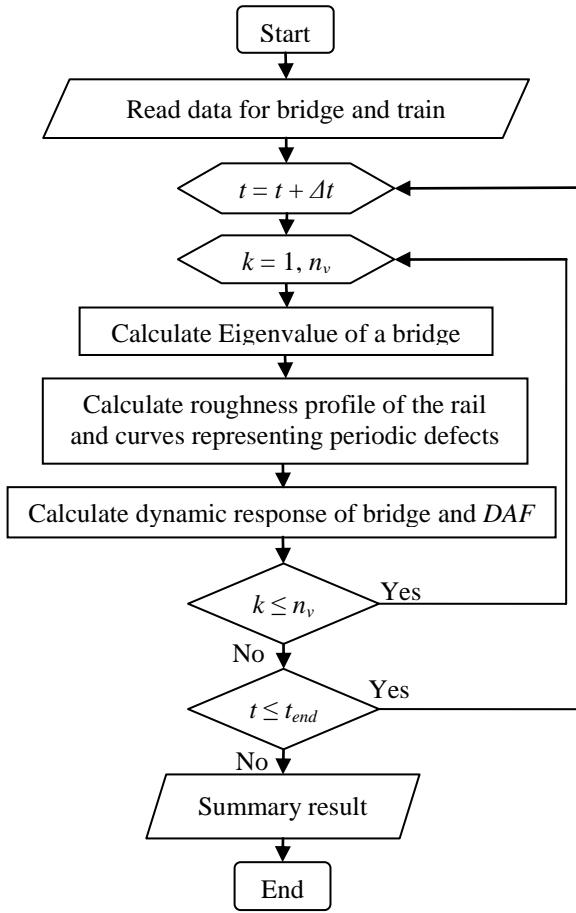


Fig. 5 An algorithm to solve the bridge–train interaction

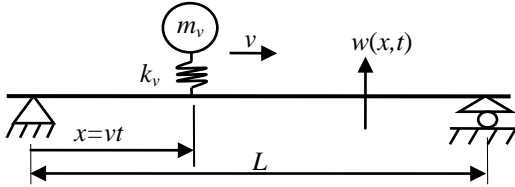


Fig. 6 Beam subjected to a moving mass-spring system

The present algorithm has been applied to calculate the non dimensional displacement at the midpoint of the beam (Fig. 7).

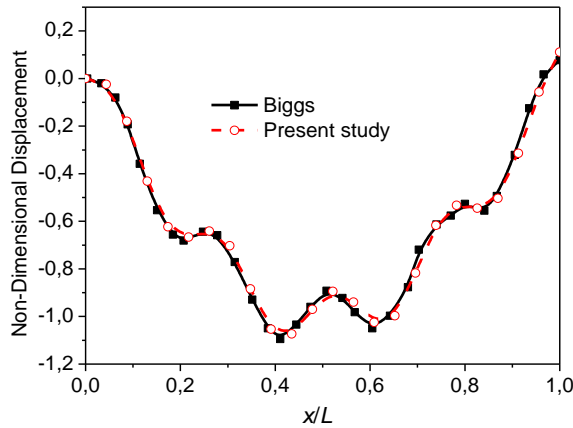


Fig. 7 The midpoint displacements of the beam

The results obtained are presented in Fig. 7 and compared to those obtained in [2]. From the comparison,

one can note that the present algorithm is in very good agreement with this reference.

4. Parametric study of the bridge-train model

The developed methodology can be used in the parametric study to predict the bridge dynamic response under moving vehicles. The train consists of identical cars and travels over a bridge. The data assumed below are close to those used in the case of high-speed train and railway bridges. The model depicted in Fig. 3 is considered with the following parameters [5]: $m_v = 12000$ kg, $k_v = 1200$ kN/m, $c_v = 10$ kN-s/m, $m_s = 5000$ kg, and $k_s = 1.e7$ N/m. The train is assumed to have five carriages. The train car length, $d = 25$ m. A simply-supported beam modeling the bridge possesses the following properties [5]: Young's modulus $E = 2.e11$ Pa, length of bridge $L = 30$ m, moment of inertia $I = 0.17238$ m⁴, masses per unit of length $m_l = 1.e4$ kg/m, and damping coefficient $\zeta = 2.5\%$. Also, the circular frequency of the bridge is obtained from the Eq. (12) as $\omega_B = 20.36$ rad/s.

4.1. Influence of the speed

Several features should be considered in the design of bridges used in high speed railways; the speed of the train is the first factor to be taken into account. In this study, the influence of train speed is studied using the present method. In modern analysis speeds go up to 500 km/h (138.88 m/s) for high-speed trains. The first natural frequency of the bridge is $f_B = 3.24$ Hz. The Eq. (19) we obtain $v_{cr1} = 81$ m/s. Similarly, the second, the third, the fourth and the sixth speeds are $v_{cr2} = 54$ m/s, $v_{cr3} = 40.5$ m/s, $v_{cr4} = 27$ m/s and $v_{cr5} = 20.25$ m/s.

The Fig. 8 simulates the passage of the train on a perfectly smooth surface with critical speeds of the vehicle.

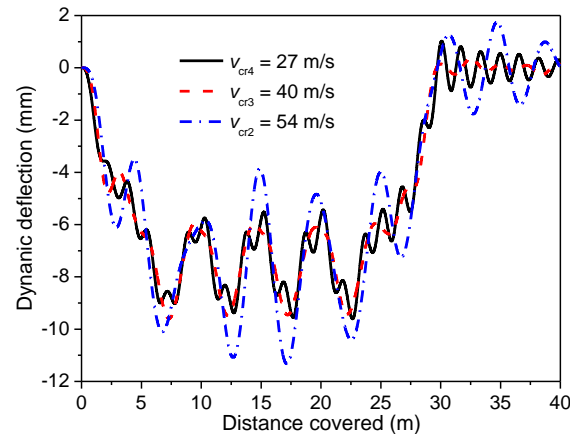


Fig. 8 The vertical central deflection of the bridge as a function of vehicle position

Fig. 9 shows the bridge deflection as a function of the frequency ratio for the perfect rail, with no roughness, no joints, nor defects. Computations are made in the interval $[0, 100]$ m/s with a step of 5 m/s ($\alpha = v/v_{cr1}$). The deflection increases with frequency ratio and reaches its maximum at $\alpha = 1.02$ ($v = 82$ m/s) which is almost coincident with $v_{cr1} = 81$ m/s. Similarly, we obtain $\alpha = 0.68$ ($v = 55$ m/s) which is almost coincident with $v_{cr2} = 54$ m/s, $\alpha = 0.37$ ($v = 29$ m/s) which is almost coincident with

$v_{cr4} = 27$ m/s, $\alpha = 0.25$ ($v = 20$ m/s) which is almost coincident with $v_{cr5} = 20.25$ m/s and $\alpha = 0.12$ ($v = 9.6$ m/s) which is almost coincident with $v_{cr6} = 10.125$ m/s. The bridge central deflection is highly dependent on the frequency parameter α .

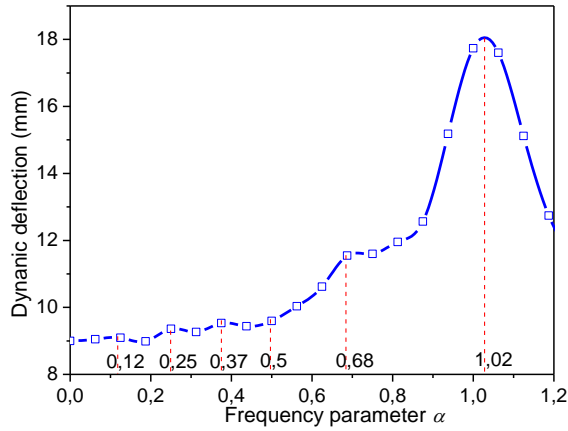


Fig. 9 Bridge central deflection as a function of the frequency parameter

4.2. Influence of rail roughness

To adequately represent the various curves of spectral concentration of power, one uses Eq. (4) with N terms. Each curve has a frequency range in which the density curve is valid. Using Eq. (4) with $N = 180$, the phase angle φ_k is randomly generated by the present method, as shown in Fig. 10.

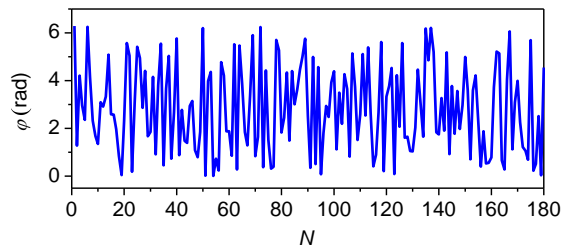


Fig. 10 Phase angle φ_k

The surface quality may be classified into several classes in terms of spectral roughness coefficient (Fig. 11).

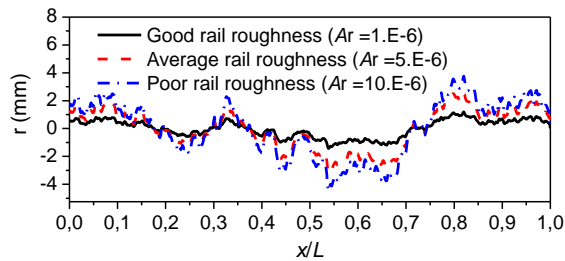


Fig. 11 Rail roughness

The Fig. 12 shows the mid-span deflection versus time t for the bridge is given for first critical speed ($v_{cr1} = 81$ m/s) with and without rail roughness. Fig. 13 shows the DAF according to the speed parameter for the perfect rail and with various values of rail roughness.

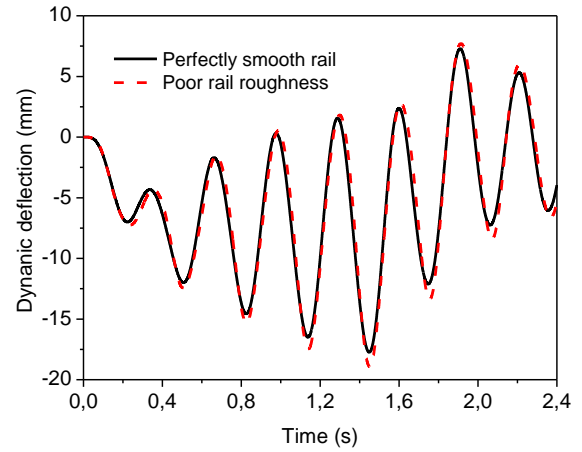


Fig. 12 Bridge central deflection for $v_{cr1} = 81$ m/s with and without roughness

For three cases of rail roughness, the rail roughness has a considerable effect on the dynamic response of the bridge, and particularly around the critical speeds. The most distinctive difference can be seen for $\alpha = 0.5$, where the difference between the good and poor profiles reaches 10.5%; followed by $\alpha = 1$, where the difference between the good and poor profiles reaches 6.9%.

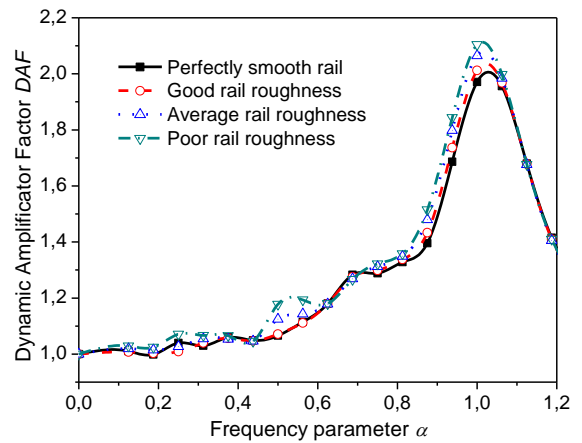


Fig. 13 DAF under four different rail roughness conditions

4.3. Influence of rail-joint

Rail-joint parameters are: joint length, $b_j = 100$ mm, distance between two joints, $A_j = 25$ m, and three cases for joint depth, $a_j = 20$ mm, 40 mm, and 60 mm. Four cases for joint position (B_j , distance between the origin and the first joint) have been considered (Fig. 14), namely $B_j = (L - A_j)/2 = L/12, L/4, L/2$ and $3L/4$.

In Fig. 15, the mid-span deflection versus time t for the bridge are given for critical speed 20 m/s (72 km/h) and $B_j = L/2$ with and without joint defect. The numerical results in Fig. 15 do not include the influence of rail roughness, only the defect of the joint is considered. From the Figs. 15 one can see that the effect of the joint defect starts from 0.75 s because the defect is located at $x = 15$ m.

This effect is significant on the dynamic response of the bridge for low speeds ($\alpha = 0$ to 0.5), see Fig. 16, it is about 25% for $\alpha = 0.125$ ($v = 10$ m/s) and of 20% for $\alpha = 0.25$ ($v = 20$ m/s). On the other hand for high speeds from $\alpha = 0.5$ to 1 ($v = 40$ to 100 m/s), the effect is unimportant it is about 2%.

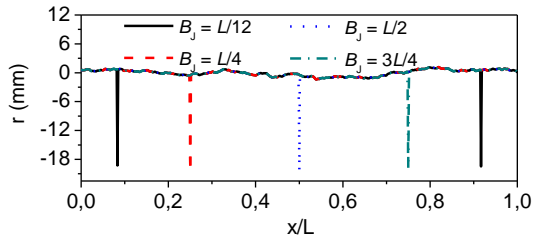


Fig. 14 Profile of the rail with good rail roughness and joint defects for 4 cases of B_J

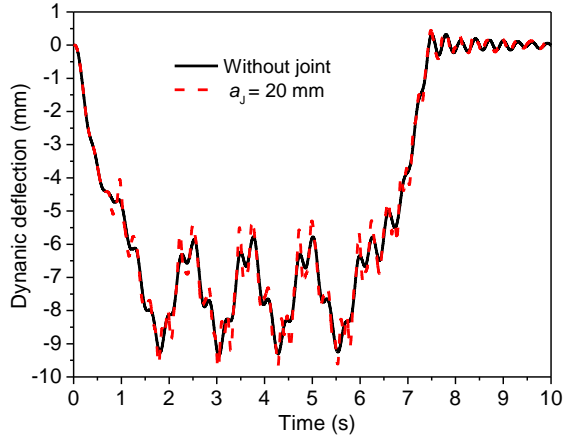


Fig. 15 Bridge central deflection for $v_{cr5} = 20$ m/s with and without joint defect

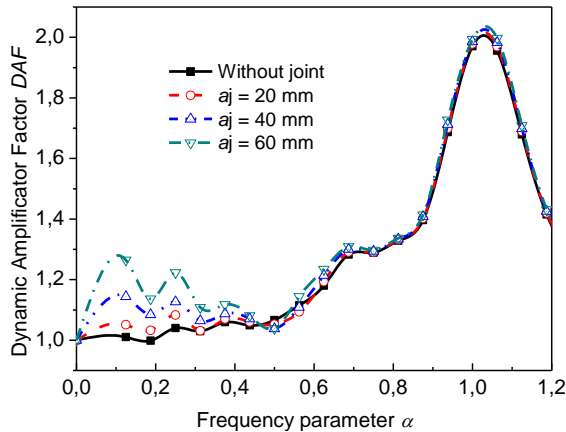


Fig. 16 DAF for $B_J = L/2$ under four different a_j conditions

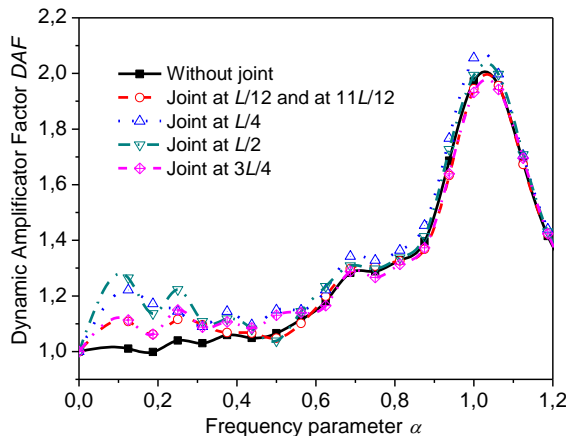


Fig. 17 DAF under four different B_J conditions

In Fig. 17 one can see the DAF for various positions of a discontinuity with a depth $a_j = 60$ mm at

$B_J = L/12$, $B_J = L/4$, $B_J = L/2$ and $B_J = 3L/4$.

It can be seen that the most favorable case is when there is a discontinuity at position $B_J = L/12$ and $B_J = 3L/4$. The most unfavorable situation is $B_J = L/2$ and $B_J = L/4$.

Finally, one can conclude that the combined effect of train loading with the presence of a rail discontinuity may be catastrophic at certain train speeds within the actual range of traveling speeds.

5. Conclusions

The dynamic responses of the bridge subjected to high-speed trains are obtained in the time domain by using the bridge-vehicle coupled model. Parameters such as the bridge deflection and especially the track irregularity with rail defects are investigated. Based on the results obtained, the following conclusions can be drawn:

1. The bridge central deflection is highly dependent on the frequency parameter α .

2. The rail roughness has a considerable effect on the dynamic response of the bridge, and particularly around the critical speeds.

3. The presence of a rail discontinuity leads to an amplitude increase. In particular, in the case when the train speed coincides with the critical speed (resonance) and especially for speeds relatively low (0 to 40 m/s) for TGV, the high-speed train.

4. One can see the DAF for various positions of a discontinuity, it can be seen that the most favorable of the cases is when there is a discontinuity at position $B_J = L/12$ and $B_J = 3L/4$. The designer must avoid placing rail discontinuities near the location $B_J = L/2$ and $B_J = L/4$ of the bridge since this is proven as the most unfavorable situation.

The combined effect of moving loads and impact caused by these irregularities may prove to be catastrophic for certain values of train speeds.

References

1. **Fryba, L.** 1999. Vibration Of Solids And Structures Under Moving Loads, Thomas Telford Ltd., London, 494 p. <http://dx.doi.org/10.1680/vosasuml.35393>.
2. **Biggs, J.M.** 1964. Introduction to structural dynamics, New York (NY, USA): McGraw-Hill.
3. **Chatterjee, P.K.; Datta, T.K.** 1995. Dynamic analysis of arch bridges under traveling loads, International Journal of Solids and Structures 32(11): 1585-1594. [http://dx.doi.org/10.1016/0020-7683\(94\)00193-Z](http://dx.doi.org/10.1016/0020-7683(94)00193-Z).
4. **Jong-Shyong Wu, Lieh-Kwang Chiang.** 2003. Out-of-plane responses of a circular curved Timoshenko beam due to a moving load, International Journal of Solids and Structures 40: 7425-7448. <http://dx.doi.org/10.1016/j.ijsolstr.2003.07.004>.
5. **Shen-Haw Ju, Hung-Ta Lin** 2008. Experimentally investigating finite element accuracy for ground vibrations induced by high-speed trains, Engineering Structures 30(3): 733-746. <http://dx.doi.org/10.1016/j.engstruct.2007.05.019>.
6. **Law, S.S.; Zhu, X.Q.** 2005. Bridge dynamic responses due to road surface roughness and braking of vehicle, Journal of Sound and Vibration 282(3-5): 805-830.

- <http://dx.doi.org/10.1016/j.jsv.2004.03.032>.
7. **Xia, H.; De Roeck, G.; Zhang, N.; Maeck, J.** 2003. Experimental analysis of a high-speed railway bridge under Thalys trains, *Journal of Sound and Vibration* 268: 103-113.
[http://dx.doi.org/10.1016/S0022-460X\(03\)00202-5](http://dx.doi.org/10.1016/S0022-460X(03)00202-5).
 8. **Yeong-Bin Yang; Jong-Dar Yau.** 1997. Vehicle-bridge interaction element for dynamic analysis, *Journal of Structural Engineering, American Society of Civil Engineers* 123(11): 1512-1518.
[http://dx.doi.org/10.1061/\(ASCE\)0733-9445\(1997\)123:11\(1512\)](http://dx.doi.org/10.1061/(ASCE)0733-9445(1997)123:11(1512)).
 9. **Kerr, Arnold D.; Cox, Joel E.** 1999. Analysis and tests of bonded insulated rail joints subjected to vertical wheel loads, *International Journal of Mechanical Sciences* 41: 1253-1272.
[http://dx.doi.org/10.1016/S0020-7403\(98\)00042-3](http://dx.doi.org/10.1016/S0020-7403(98)00042-3).
 10. **Henchi, K.; Fafard, M.; Talbot, M.; Dhatt, G.** 1998. An efficient algorithm for dynamic analysis of bridges under moving vehicles using a coupled modal and physical components approach., *Journal of Sound and Vibration* 212(4): 663-683.
<http://dx.doi.org/10.1006/jsvi.1997.1459>.
 11. **Press, W.H.; Teukolsky, S.A.** 1992. Portable random number generators, *Computers in Physics* 6: 522-524.
 12. **Bayat, M.; Barari, A.; Shahidi, M.** 2011. Dynamic response of axially loaded Euler-Bernoulli beams, *Mechanika* 17(2): 172-177.
<http://dx.doi.org/10.5755/j01.mech.17.2.335>.
 13. **Jiang, R.J.; Au, F.T.K.; Cheung, Y.K.** 2004. Identification of vehicles moving on continuous bridges with rough surface, *Journal of Sound and Vibration* 274: 1045-1063.
[http://dx.doi.org/10.1016/S0022-460X\(03\)00664-3](http://dx.doi.org/10.1016/S0022-460X(03)00664-3).
 14. **Augustaitis, V.K.; Gičan, V.; Šešok, N.; Iljin, I.** 2011. A reduction of the equations of the linear stationary vibrating systems without limitations of dissipation using the method of modal truncation, *Mechanika* 17(5): 510-517.
<http://dx.doi.org/10.5755/j01.mech.17.5.728>.
 15. **Newmark, N.M.** 1970. A Method of computation for structural dynamics, *American Society of Civil Engineers, Journal of Engineering Mechanics Division* 85(EM3): 67-94.
 16. **Fryba, L.** 2001. A rough assessment of railway bridges for high speed trains, *Engineering Structures* 23: 548-556.
[http://dx.doi.org/10.1016/S0141-0296\(00\)00057-2](http://dx.doi.org/10.1016/S0141-0296(00)00057-2).

Y. Khadri, S. Tekili, E. M. Daya, A. Daouadji, B. Merzoug

BĖGIŲ SUJUNGIMŲ IR TRAUKINIŲ KRITINIO GREIČIO ĮTAKA TILTŲ DINAMIKAI

Re z i u m ė

Geležinkelio tiltų dinaminių procesų intensyvėjimas pervažiauvus sąstatui priklauso nuo įvairių veiksnių. Tai gali būti bėgių paviršiaus nelygumai, bėgių tarpusavio sujungimai ir t. t. Šie defektai paprastai turi įtakos sąstato ir tilto tarpusavio sąveikai. Šiame darbe bėgių sujungimų defektų įtaka siejama su sąstato kritiniu greičiu. Bėgių sujungimai modeliuojami atsižvelgiant į periodinius nukry-

pimus nuo normos. Tiltas modeliuojamas kaip atremta pastovaus skerspjuvio sija. Traukinys modeliuojamas kaip pastoviu greičiu judanti vagonų vilkstinė. Pagrindinių tilto ir traukinio judėjimo lygčių sistema išvesta pritaikant Lagranžo ir formų superpozicijos techniką. Šios lygtys skaitmeniškai integruojamos Njumarco metodu. Straipsnyje pateikta programa FORTRAN paminėtų defektų įtakos tilto dinamikai analizei atlikti.

Y. Khadri, S. Tekili, E. M. Daya, A. Daouadji, B. Merzoug

EFFECTS OF RAIL JOINTS AND TRAIN'S CRITICAL SPEED ON THE DYNAMIC BEHAVIOR OF BRIDGES

S u m m a r y

The dynamic amplification of the railway bridges caused by the passage of a train varies according to several factors. Among these factors: defaults of roughness of the rail and its joints, etc. These defects are usually encountered in railways and they influence the dynamics of the vehicle-bridge interaction, whence the importance of this study. In this paper, the defect of rail joint is investigated with train's critical speed. The joints between the rails are modeled by periodic irregularities. The bridge is modeled by a simply supported uniform beam. The train is modeled as a convoy of vehicles moving with a constant speed. The governing equations of motion for the bridge-train interaction system are derived using the Lagrangian formulation and the modal superposition technique. These equations are integrated numerically by applying the Newmark method. This paper presents a computation code in FORTRAN to analyze the effect of the above-mentioned defects on the bridge's dynamic response.

Keywords: bridge dynamics, rail roughness, rail joint, critical speed, dynamic amplification factor.

Received September 13, 2011

Accepted December 19, 2012